Journal of Physics: Conference Series **244** (2010) 022041 doi:10.1088/1742-6596/244/2/022041

Magnetic Collimation Of Petawatt Driven Fast Electron Beam For Prospective Fast Ignition Studies

S. Kar, D. Adams, M. Borghesi, K. Markey, B. Ramakrishna, M. Zepf
School of Mathematics and Physics, Queen's University, Belfast, BT7 1NN, U.K.

K. Lancaster, P. Norreys, A.P.L. Robinson
Central Laser Facility, Rutherford Appleton Laboratory, Chilton, OX11 0QX, U.K.

D.C. Carroll, P. McKenna, M. Quinn, X. Yuan
Department of Physics, University of Strathclyde, Glasgow, G4 0NG, U.K.

C. Bellei, J. Schreiber
Blackett Laboratory, Imperial College London, London SW7 2BZ, U.K.

E-mail: s.kar@qub.ac.uk

Abstract. Collimated transport of fast electron beam through solid density matter is one of the key issues behind the success of the fast ignition scheme by means of which the required amount of ignition energy can be delivered to the hot spot region of the compressed fuel. Here we report on a hot electron beam collimation scheme in solids by tactfully using the strong magnetic fields generated by an electrical resistivity gradient according to Faraday's law. This was accomplished by appropriately fabricating the targets in such a way that the electron beam is directed to flow in a metal which is embedded in a much lower resistivity and atomic number metal. Experimental results showed guided transport of hot electron beam over hundreds of microns length inside solid density plasma, which were obtained from two experiments examining the scheme for petawatt laser driven hot electron beam while employing various target configurations.

1. Introduction

Achieving collimated transport of fast electrons through solid density plasmas is a hot topic because of its relevance for fast ignition (FI) [1, 2], high energy density physics [3], laser induced radiation sources [4] and particle acceleration [5]. Experimental studies, via laser and target parameter scans, on hot electron transport in solids show minimum spray angle of 30-40 degrees [6, 7, 8] - which limits the efficiency with which energy can be coupled to the hot spot in FI. Therefore various schemes are being investigated in order to achieve less divergent or even collimated transport. In addition to the ideas such as the cone [9] and the wire [10] guiding, recent theoretical studies proposed a concept based on self-generated magnetic fields at resistivity boundaries [11]. Combining Ohm's law with Faraday's law one obtains $\frac{\partial \mathbf{B}}{\partial t} = \eta \nabla \times \mathbf{J}_f + (\nabla \eta) \times \mathbf{J}_f$,

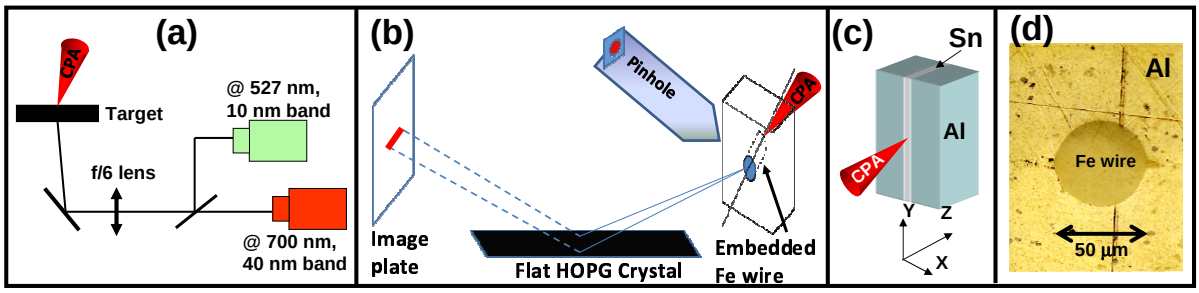

Figure 1. **(a)** and **(b)** show schematics of the setups in the experiments, EXP-1 and EXP-2 respectively. **(c)** Schematic of the target with one dimensional guiding geometry.**(d)** shows the image of the transverse cross-section of the target of two dimensional guiding geometry taken by an optical microscope.

where η is the resistivity($\propto Z/T_e^{1.5}$ in the Spitzer limit) and $\mathbf{J}_f$ is the density of the fast electron current flowing into the target. The second term on the right hand side of this equation tells about the generation of magnetic field due to a resistivity gradient which pushes fast electrons towards regions of higher resistivity. Once established, this field is further enhanced by magnetic field due to the current density gradient. Simulations have shown that for the parameters of the Vulcan PW, the field strength is sufficient to collimate an MeV electron beam [11]. One key point for experiments, where the targets are initially cold, is to maintain the sign of the resistivity gradient across the Z-boundary as the target heats up to hundreds of eV during the interaction. This can simply be achieved by using a core material (in which the electron beam is intended to be confined) with a higher Z and higher initial core resistivity than the surrounding medium.

The experimental proof of principle of the magnetic collimation scheme was carried out at Vulcan Petawatt laser facility employing one dimensional structured target [12], where the role of strong magnetic field at the resistivity gradient is proved by the help of computer simulations. In a follow-on experiment at the same facility and employing hard X-ray diagnostics, we extended our studies further with the same one dimensional as well as two dimensional guiding configurations - targets exhibiting a core/cladding structure analogous to optical waveguides, where fast electrons were forced to propagate inside a thin ($\sim$ 50 μm diameter) Iron wire of higher electrically resistivity and atomic number than the aluminum in which it is embedded.

2. Experimental setup

Both of the experiments (let us call the first proof-of-principle experiment as 'EXP-1' and the follow-on experiment as 'EXP-2' - schematics of the setups are shown in the figure. 1(a) and (b) respectively) were performed at Rutherford Appleton Laboratory employing Vulcan Petawatt laser system. After reflection from a plasma mirror, which was employed in order to reduce the prepulse and amplified spontaneous emission intensities on the target, the laser pulse delivered 150 J of energy on target in fwhm duration of 1 ps. Laser spot size on the target was 20 μm, reaching peak intensity of $\sim 10^{20}$ W/cm^2 on target at near normal incidence. A schematic of the one dimensional electron guiding target fielded in the experiments is shown in the figure 1(c). The CPA was targeted to irradiate the embedded 12 μm thick Tin (Sn) layer sandwiched between two Aluminium (Al) slabs. The target thickness was 200 μm. In case of the target for cylindrical guiding fielded in EXP-2, Fe wire of 50 μm diameter was embedded in Al, and the target thickness was 250 μm. An optical microscope image of transverse cross-section of the target is shown in figure 1(d). The materials were chosen based on the contrast of their

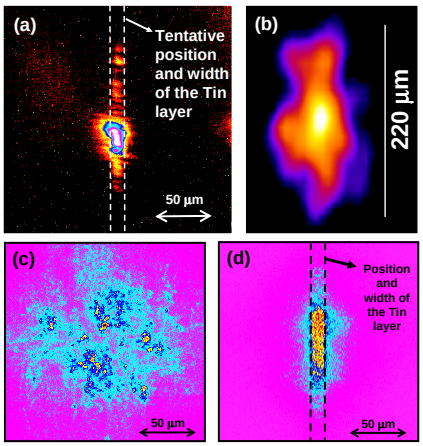

Figure 2. **(a)** and **(b)** are respectively the time integrated image of optical transition radiation and X-ray pinhole camera image of the Al-Sn-Al one dimensional guiding target (shown in Fig 1(a)) rear surface obtained in EXP-1 and EXP-2, respectively. **(c)** and **(d)** shows 2D spatial distribution of square of the hot electron density at the rear surface a 200 μm thick Al foil target and the guiding target, as employed in the experiment, obtained from 3D hybrid code described in the text.

atomic weights and electrical resistivities, as well from the point of view of fabrication. In the EXP-1, the target rear surface was lapped to a roughness of 50 nm rms and was gold coated (of sub micron thickness) and in EXP-2, 15 μm Cu foil was glued to the target rear surface. In the EXP-1, time integrated images of the optical transition radiation (OTR) at 527±5 nm and Plankian emission at 700±20 nm wavelengths (using bandpass optical filters) from the target rear surface were simultaneously recorded by CCD cameras. The spatial resolution of the images at 527 nm and 700 nm were 4 μm and 5.5 μm respectively. In the EXP-2, the electron beam size at the target rear surface was diagnosed by Xray diagnostics such as HOPG (highly oriented pyrolytic graphite) spectrometer [13] and pinhole camera, mainly looking at 8.05 KeV X-rays from the Cu tracer layer at the target rear surface due to K-α transitions in Cu by the hot electrons passing through it.

3. Results

According to the Faraday's law, the magnetic field is created across the resistivity gradient, which is not limited to any specific symmetry. Therefore, strong resistivity gradient along the Al-Sn boundary will lead to a rapid magnetic field growth and consequently guiding of the fast electrons should still occur in the target with one dimensional guiding geometry (as shown in figure 1(a)), albeit the fast electrons will only be strongly confined in one dimension normal to the Sn slab. Indeed, we obtained elucidating results showing the effect of the strong collimating resistive magnetic field while employing one dimensional guiding targets in both experiments. Highly elliptical shape of the hot electron beam distribution across the one dimensional guiding target rear surface is inferred from the OTR and X-ray pinhole images obtained from the EXP-1 and EXP-2 respectively, shown in the figure 2 (a) and (b) respectively. It is striking to see the oblong shape, width and the orientation of the image in the experimental data which correlates very well with the sandwiched Tin layer of the guiding target and contrasts with the typical circular patterns obtained from flat foil targets [6, 7]. Weaker magnetic confinement parallel to the Sn slab, as compared along normal to the tin layer, should result in an elongated electron beam profile at the target rear surface.

Simulations ware carried out to study the hot electron beam transport in the presence of resistive boundaries by modeling the 1D guiding geometry [12]. 3D hybrid code, called ZEPHYROS [11], was employed which uses similar approximations and methods to the hybrid code of Davies [14], i.e. a particle-based hybrid code with static background plasma. As expected, the simulation for the pure Al target produced a fairly uniform electron distribution of 100 μm fwhm at the rear surface (i.e. across the z =200 μm plane) as shown in the figure 2(c). On the other hand, the asymmetrical electron distribution obtained for the case of sandwich

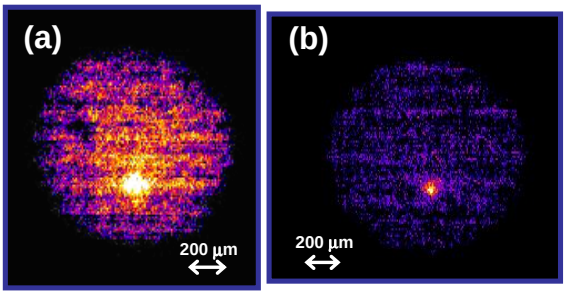

Figure 3. **(a)** and **(b)** are respectively the Xray pinhole camera images of the rear surface of 250 μm thick Fe foil and Al-Fe-Al two dimensional guiding target (shown in Fig 1(b)) obtained in EXP-2.

target can be seen in figure 2(d). Due to the resistivity gradient across the interfaces, the strong magnetic walls generated at the interfaces confine electrons within it, whereas some of the electrons managed to escape before the strength of the magnetic field could be sufficient to confine them. The simulation also reproduces the ratio between the number of electrons escaped to the number of electrons confined along the X axis (the collimation axis), thus establish the underlying dynamics of the magnetic field. The experimentally obtained heating profile of the target rear surface provided further evidence of collimated electron flow in the target [12]. While employing the 2D collimator target in EXP-2, we found a clear reduction in the electron beam size at the target rear surface as compared to the reference Fe target of same thickness (see figure 3).

4. Conclusion

It is experimentally demonstrated that the divergence of hot electrons inside a solid density target can be controlled by targets with suitable resistivity gradients around the beam. The resistivity gradients at the interfaces are practically maintained, for the relevant time scale, by choosing central metal of higher atomic number as well as higher electrical resistivity than the surrounding one. This scheme may have substantial positive impact on the Fast Igniter approach to fusion energy production, by enhancing coupling efficiencies of the relativistic electron beam to the fusion fuel and by relaxing some geometrical constraints on the target design.

5. Acknowledgements

The authors would like acknowledge funding support from (Engineering and Physical Science Research Council (EPSRC) and the Royal Society, UK and support for target fabrication from the QUB mechanical workshop.

References

[1] M. Tabak *et al.*, Phys. Plasmas, **12**, 057305 (2005).
[2] S. Nakai and K. Mima, Rep. Prog. Phys., **67**, 321 (2004).
[3] E.M. Campbell, Nucl. Instrum. methods A, **415**, 27 (1998).
[4] H.S. Park *et al.*, Phys. Plasmas, **13**, 056309 (2006).
[5] M. Borghesi *et al.*, Fusion Sci. Tech., **49**, 412 (2006).
[6] R.B. Stephens *et. al.*, Phys. Rev.E, **69**, 066414 (2004).
[7] J.J. Santos *et. al.*, Phys. Rev. Lett. **89**, 025001 (2002).
[8] K. Lancaster *et al.*, Phys. Rev. Letts., **98**, 125002 (2007).
[9] R. Kodama *et al.*, Nature, **432**, 1005 (2004).
[10] J.S. Green *et al.*, Nature Phys., **3**, 853 (2007).
[11] A.P.L. Robinson *et al.*, Phys. Plasmas, **14**, 083105 (2007).
[12] S. Kar *et. al.*, Phys. Rev. Letts., **102**, 055001 (2009)
[13] A.W. Moore, *Highly oriented pyrolytic graphite, Chemistry and Physics of Carbon*, Vol. 11, Marcel Dekker, New York, 1973.
[14] J. Davies, Phys. Rev. E, **65**, 026407 (2002).
[15] S.C. Wilks *et al.*, Phys. Rev. Letts., **69**, 1383 (1992).